EFFECT OF IRRADIATION ON TOUGHNESS-TEMPERATURE CURVES IN V-4CR-4TI

— E. Donahue, G. R. Odette, G. E. Lucas, and J. W. Sheckherd (University of California, Santa Barbara); A. Rowcliffe (Oak Ridge National Lab)

OBJECTIVE

The objective of this work is to explore the variation of effective fracture toughness with test temperature in V-based alloys, and to assess the effect of neutron irradiation on this toughness-temperature relationship.

SUMMARY

Small, pre-cracked, 1/3-sized Charpy specimens of V-4Cr-4Ti were irradiated to a dose of 0.5 dpa at a temperature of 200 ± 8 °C. The specimens were tested in three point bending under static conditions to measure effective toughness-temperature curves. Fracture processes were examined by using confocal microscopy and fracture reconstruction methods. It was found that this alloy undergoes normal stress-controlled cleavage transition below a characteristic temperature, and that irradiation hardening increased the transition temperature significantly. Shifts in the transition temperature imposed by irradiation hardening can be reasonably predicted by a simple equivalent yield stress model.

PROGRESS AND STATUS

Introduction

Vanadium alloys are attractive candidates for structural applications in fusion reactors because of their low neutron activation, favorable thermal properties and potential for radiation stability. However, a potential problem that these alloys share with other body centered cubic (bcc) metals is a transition in fracture mode from ductile to brittle cleavage transition below a temperature (T_t), with an attendant loss in fracture toughness. Moreover, T_t may be significantly elevated as a consequence of irradiation. Preliminary studies using nonstandard tests — including one-third-size Charpy V-notch and disc bend specimens — have suggested that alloy compositions in the range V-4Cr-4Ti are highly resistant to embrittlement, with T_t in the vicinity of or below -196°C [1-5].

However, T_t depends on the details of the test procedure[6], and it cannot be used to quantify structural stress and strain limits; hence, it is neither a fundamental material property nor a useful engineering parameter. A more useful quantitative measure of fracture resistance is the effective toughness as a function of temperature, $K_e(T)$; however, this too depends on variables such as size scales and flaw geometry, loading rate, irradiation and other sources of embrittlement (e.g., hydrogen). As discussed in detail elsewhere[7], it may be possible to develop a method to predict the stress and strain limits of flawed fusion structures using a $K_e(T)$ curve adjusted on an absolute temperature scale using measured shifts to account for variables such as irradiation, constraint, and strain rate. Hence, in support of this approach the objective of this study was to examine the effects of irradiation on the $K_e(T)$ of a V-4Cr-4Ti alloy, and to evaluate these effects within the context of understanding the mechanisms of fracture and the effects of irradiation on these mechanisms in this alloy system.

Experiment

The study was carried out on a 3.8 mm thick plate in the 40% warm-rolled (400°C) condition taken from the program heat of V-4Cr-4Ti (#832665) [8]. Small, 1/3-sized Charpy V-notch specimens (3.33 x 3.33 x 25.4 mm) were electro-discharge machined from the plate. The machined specimens were annealed for 2h at 1000°C in a vacuum of better than 10^{-4} Pa to produce a recrystallized microstructure and remove residual hydrogen. This series of heat treatments produces an average grain size of about 25 μm and a Vickers microhardness of about 150±5 [9,10]. Fatigue pre-cracking was carried out at a final $\Delta K \leq 15$ MPa√m to a nominal crack length (a) to specimen width (W) ratio of $a/W \approx 0.5$. The specimens were encapsulated and irradiated in the High Flux Beam Reactor (HFBR) to a dose of 0.5 dpa at 200±8 °C.[14]

Following irradiation, the specimens were tested in three point bending over a temperature range from -60 to 20°C at approximate loading rates of 2.5×10^{-6} m/s. Load and load-line displacement were monitored during testing. In most cases a cleavage pop-in occurred after some permanent displacement. In most of the pop-in cases, the specimen was post-test fatigued to mark the final location of the pop-in. In all these cases K_e was determined from

$$K_e = \sqrt{J_{Ie}E'} \qquad (1)$$

where E' is the plane strain elastic modulus and J_{Ie} is the effective energy release rate determined from the area under the stress-displacement curve up to the load drop at cleavage pop-in. In several cases, a maximum load was exhibited without pop-in, and corresponding fractography indicated subcritical crack growth; in these cases K_e was also determined from equation (1), but J_{Ie} was determined from the area under the stress-displacement curve up to maximum load. Finally, the specimen tested at 20°C exhibited no pop-in and no maximum load before the test was terminated. In this case, J_{Ie} was taken from the total area under the stress-displacement curve.

Following testing, specimen fracture surfaces were examined by both scanning electron microscopy (SEM) and confocal microscopy (CM). As described elsewhere [11,12], the CM images can be used to obtain quantitative, three-dimensional topographs of conjugate fracture surfaces. These topographs can be used with fracture reconstruction (FR) methods to determine the sequence of events in front of the crack tip ultimately leading to macroscopic fracture (e.g., a macroscopic pop-in). The post-pop-in fatigue crack provides an additional reference to improve the alignment of images in FR. The CM/FR method also provides a measure of the critical crack tip opening δ^* at the point of initiation of crack extension, from which an effective toughness $K_{e\delta}$ can be estimated by

$$K_{e\delta} = \sqrt{2\delta^* \sigma_y E'} \qquad (2)$$

where σ_y is the yield stress. [11,12]

Tensile tests were also performed on unirradiated and irradiated specimens of this same alloy and the results have been reported elsewhere. [13,14]

Results

Figure 1 summarizes the $K_e(T)$ data for the irradiated materials and compares these data to the trend line for the unirradiated material tested under similar conditions [13]. As can be seen, in the irradiated material K_e transitions from a lower shelf value of about 30 MPa√m to a value of about 160 MPa√m over a fairly narrow temperature range of about -30± 10°C. This is about 170°C higher than the unirradiated data trend. As noted previously, at room temperature the irradiated specimen did not fracture, but merely deformed to maximum displacement in the test fixture with a corresponding lower bound $K_{e,min}$ value of about 145 MPa√m. As shown in Figure 1, specimens primarily failed by cleavage pop-in in the lower shelf and transition regime, but in several instances the load-displacement curves showed a maximum load without a pop-in, indicative of subcritical crack growth. Indeed, both types of behavior were exhibited at the same test temperature, reflecting the statistical variability in fracture mode in the transition regime.

Figures 2-4 show representative results for selected test temperatures that corroborate some of the observations noted above. Each figure provides: 1) a load displacement trace from the mechanical test and the corresponding point on the $K_e(T)$ plot; 2) a side view and 3) a top view of the sequence of events ahead of the crack front determined from CM/FR; and 4) an SEM micrograph from a region of interest.

Figure 2 shows results for one of the tests at -30°C. In this case, the load displacement trace showed a load drop at maximum load, with a K_e of 160 MPa√m. The SEM fractography showed the formation of a cleavage pop-in corresponding to this load drop. The CM/FR images show side views of the fracture surface overlaps (shaded regions being separated) and top views of the crack plane (again shaded regions being separated and white intact) at several values of δ.

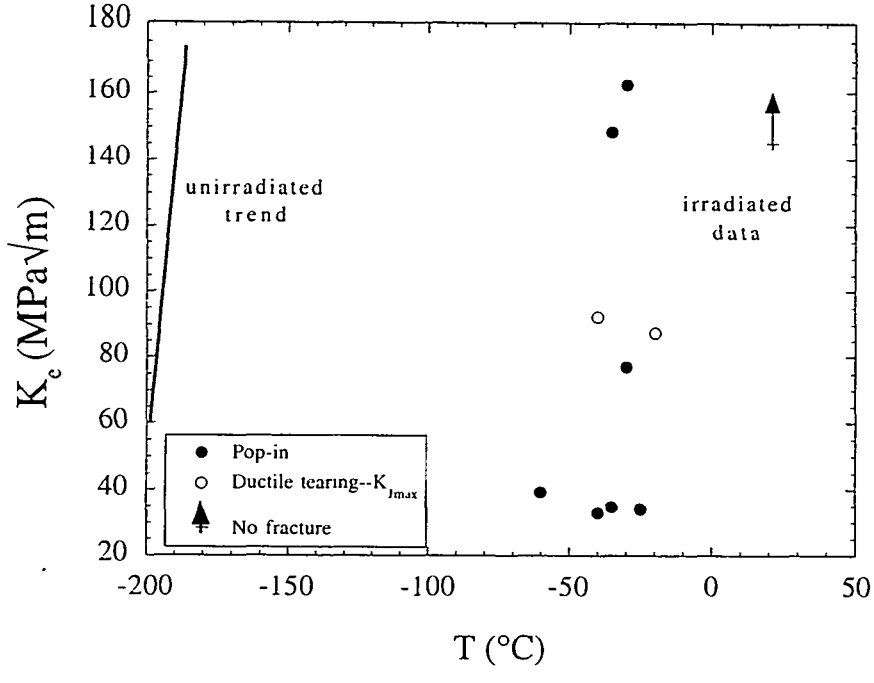

Figure 1 Variation of K_e with test temperature for irradiated and unirradiated V-4Cr-4Ti.

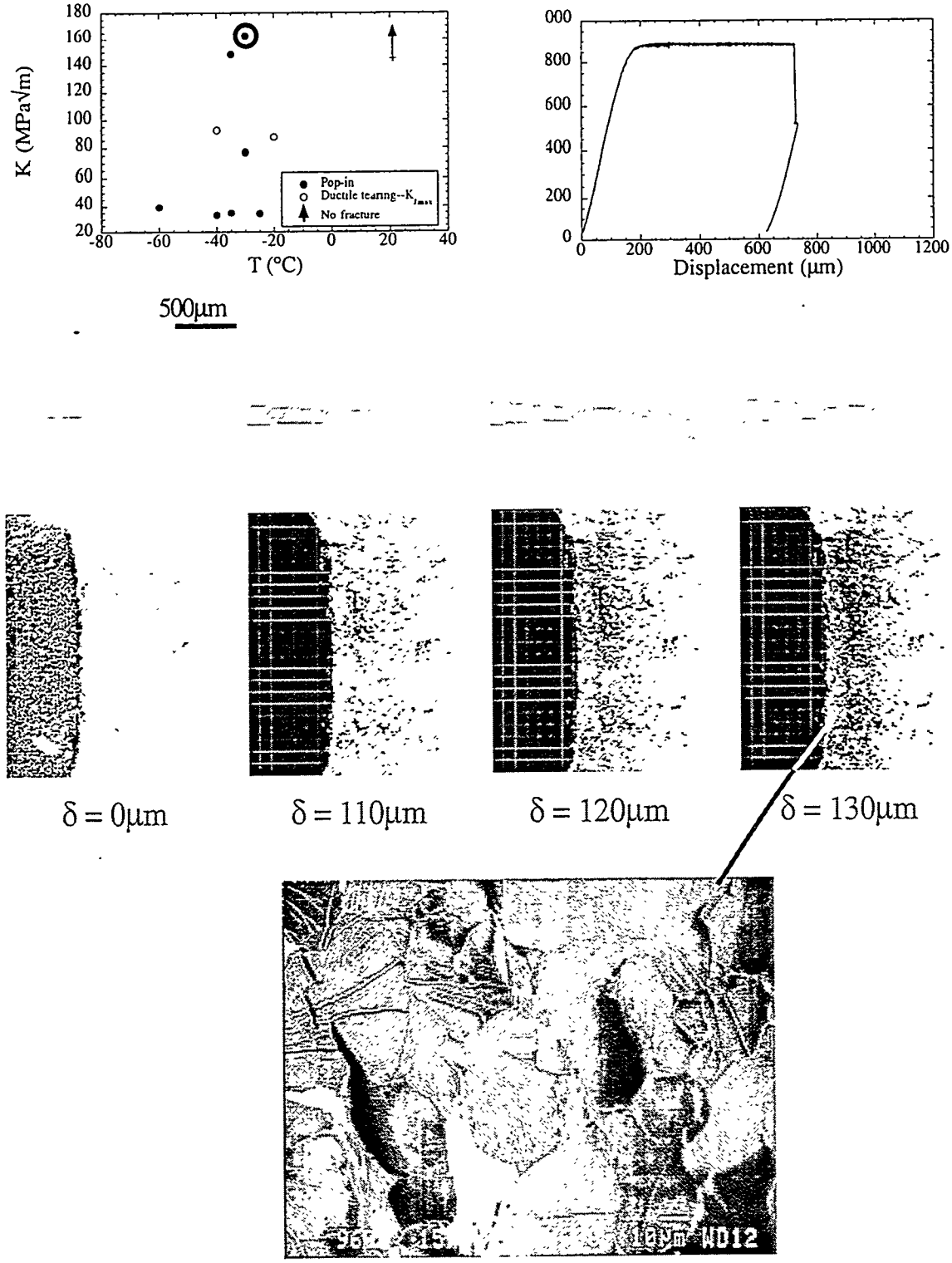

Figure 2 Load-displacement curve, CM/FR results and representive SEM micrograph for a specimen tested at -30°C.

These show that the pop-in was preceded by the formation of microcleavage cracks ahead of the crack tip; these microcracks accumulate in a single process zone and coalesce to form the pop-in at a δ^* of about 125 μm corresponding to a $K_{e\delta}$ of 168 MPa√m. SEM in the pop-in region shows well-formed cleavage facets with some out-of-plane fissures and little or no evidence of intergranular fracture.

Figure 3 shows results for a second test at -30°C. In this case, the load displacement trace shows two load drops, the first occurring before maximum load after substantially less displacement than that shown in Figure 2; the corresponding K_e was about 75 MPa√m. Again the CM/FR showed the initial formation of microcleavage cracks ahead of the crack tip, which accumulate in approximately three process zones; microcrack coalescence to form the pop-in occurred at a δ^* of about 30 μm corresponding to a $K_{e\delta}$ of 82 MPa√m. The SEM micrograph shows the well formed interface between the cleavage facets in the pop-in region and the post-pop-in fatigue crack.Figure 4 shows results for the test at -20°C. In this case, the load displacement trace exhibited a maximum, indicative of subcritical crack growth, and the test was terminated after about 1000μm of displacement; the corresponding $K_{e,max}$ obtained at the maximum load was about 90 MPa√m. The SEM and CM/FR indeed showed two regions of subcritical crack growth at the flanks of the pre-crack front, with crack initiation occurring at a δ^* of about 35 μm corresponding to a $K_{e\delta}$ of 87 MPa√m. The SEM micrograph taken from one of these regions shows discrete steps along the crack front, perhaps indicative of localized plastic flow.

As shown in Figure 5, the values of K_e measured from the load-displacement data were in very good agreement with the values of $K_{e\delta}$ determined from CM/FR.

Discussion

Cleavage fracture is believed to occur in this alloy system (as well as other bcc systems) when the tensile stresses ahead of a crack tip exceed some critical value (σ^*) over a sufficiently large area (A^*) [11,12,15]. Hence, σ^*/A^* are local measures of toughness that are intrinsic to the material and its microstructure. Since the peak stresses σ_t ahead of a crack tip are some multiple M of the yield stress, where M reflects the degree of constraint imposed by the specimen size and crack geometry, the onset of cleavage requires sufficiently low temperatures for $\sigma_t = M\sigma_y$ to exceed σ^*. Hence, increasing σ_y (e.g., by irradiation hardening or strain rate) results in the onset of cleavage at higher temperatures; and decreasing M (for instance by decreasing specimen size or notch/crack acuity decreases T_t. Indeed, the previously reported low transition temperatures in the V-4Cr-4Ti system are consistent with a relatively low σ_y in the unirradiated material combined with specimen sizes and geometries with low M.

If — as is the case for bcc steel alloys [11,15] — σ^* and A^* are relatively insensitive to temperature, strain rate and the fine scale damage imposed by irradiation, a simple way to model shifts in a reference transition temperature (ΔT_r) due to irradiation hardening (or loading rate) is to define transition temperatures at an *equivalent* reference yield stress $\sigma_{y,ref}$. The appropriate reference condition is near the highest temperature of elastic cleavage fracture, here about $K_e = 60$ MPa√m. Hence, ΔT_r can be modeled from a knowledge of the dependence of σ_y on temperature, irradiation and strain rate. For instance, assuming that the overall constitutive relation $\sigma(\varepsilon)$ for different temperatures, strain rates and levels of irradiation hardening ($\Delta\sigma_i$) are similar if the σ_y are the same, and that $\Delta\sigma_i$ is independent of temperature and strain rate, the effects of irradiation on shift can be predicted from $\Delta\sigma_i$ by an equivalent yield stress model (EYSM) as follows.

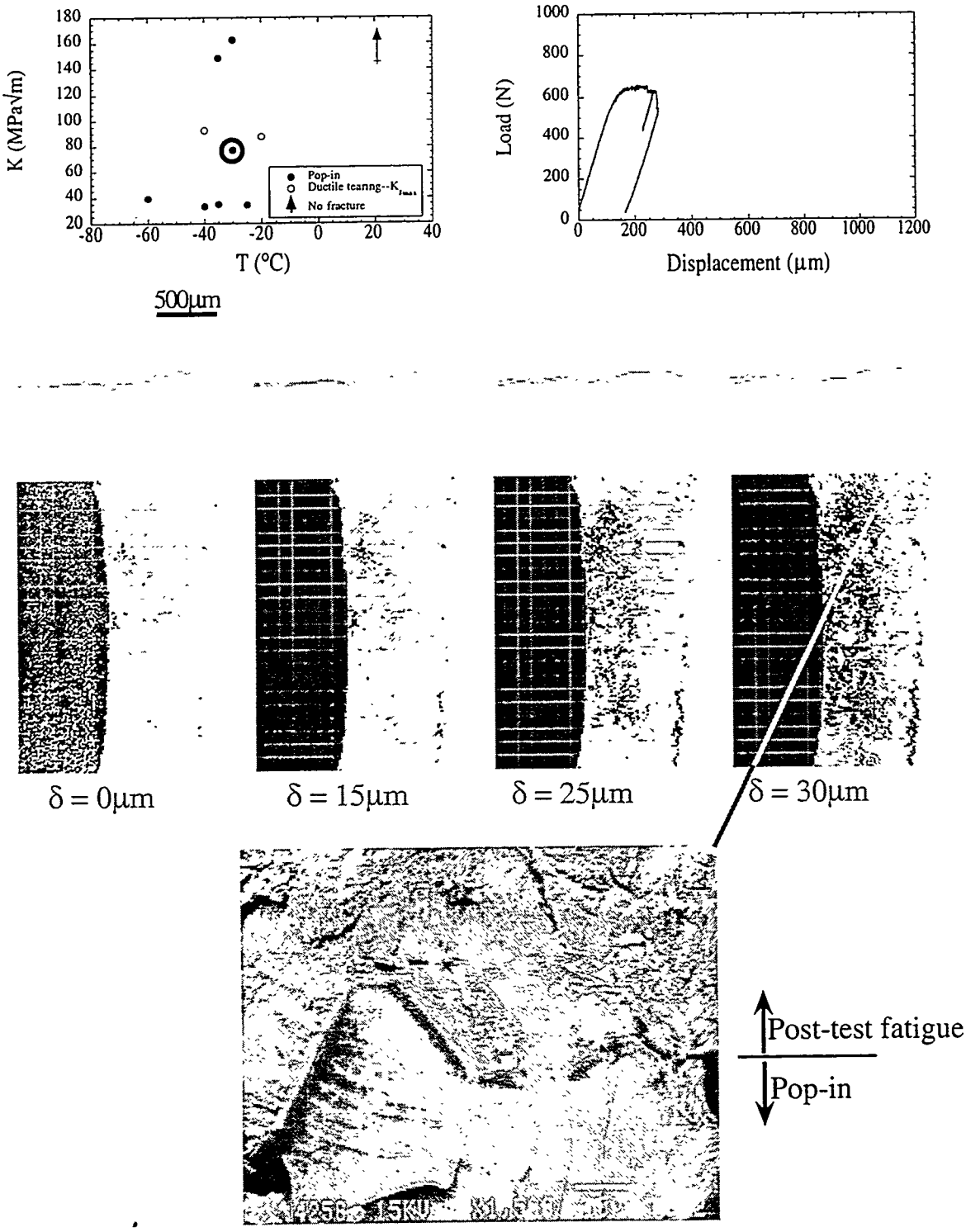

Figure 3 Load-displacement curve, CM/FR results and representive SEM micrograph for a second specimen tested at -30°C.

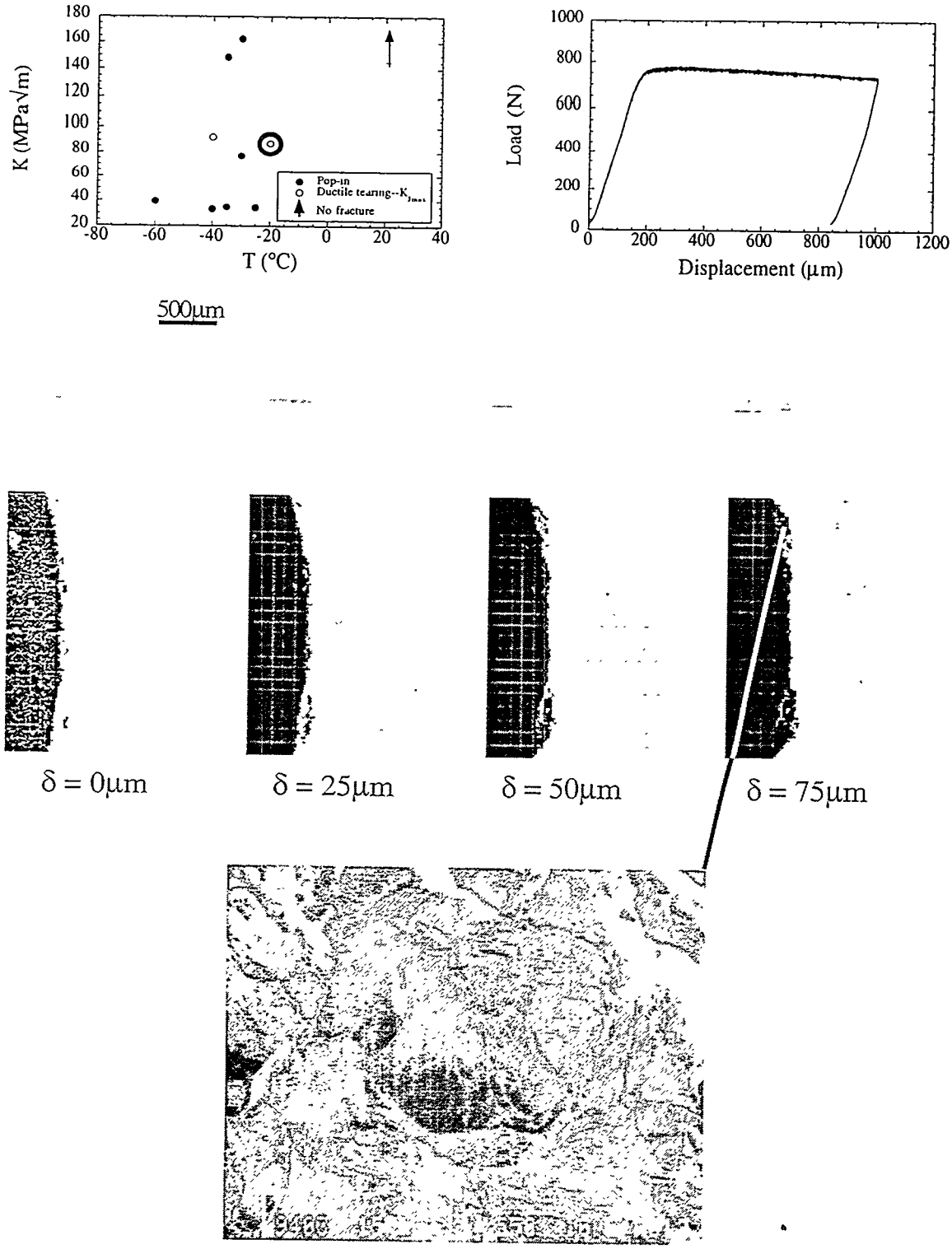

Figure 4 Load-displacement curve, CM/FR results and representive SEM micrograph for a specimen tested at -20°C.

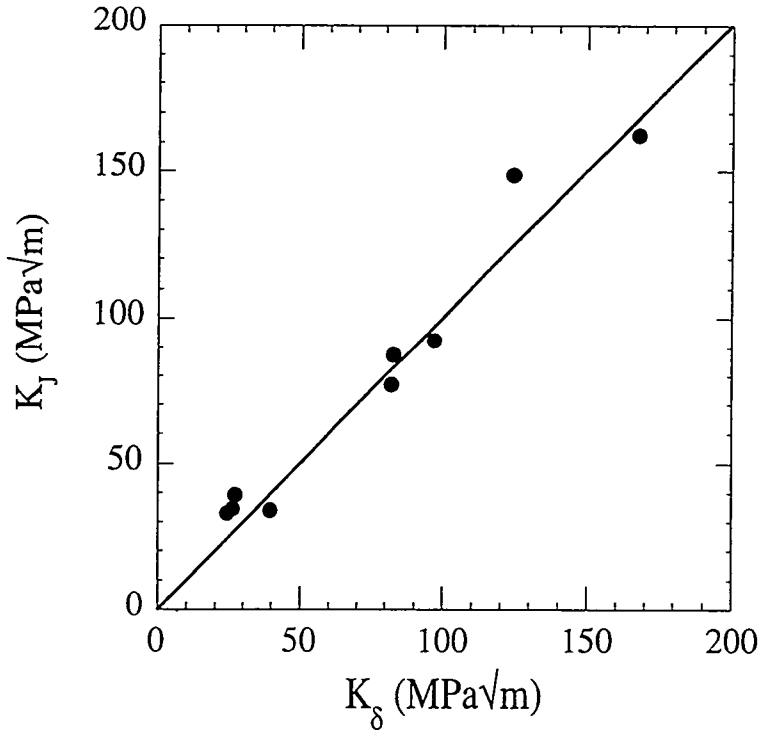

Figure 5 Comparison of K_e determined from load-displacement data with $K_{e\delta}$ determined from CM/FR.ith

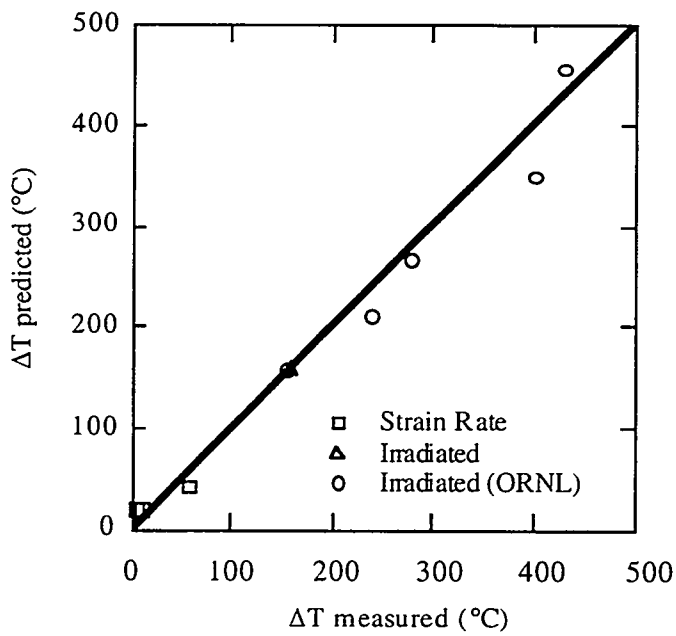

Figure 6 Comparison of measured transition temperature shifts and shifts predicted by the equivalent yield stress model.

$$\Delta T_r = T_{ri} - T_{ru}, \text{where } \sigma_{yi}(T_{ri}) = \sigma_{yu}(T_{ru}) + \Delta\sigma_i \qquad (3)$$

and the "u" and "i" subscripts refer to the unirradiated and irradiated condition, respectively.

Using the irradiation hardening results obtained for this alloy from previous work [16], estimates of ΔT_r were obtained from equation (3); and these are compared to values measured in this study in Figure 6. Also shown for comparison are the measured and predicted values of ΔT_r for other irradiation conditions of the same alloy reported by Alexander and Snead [16], and for the effects of strain rate on shift determined from static and dynamic data previously reported for this alloy [13]. In the latter case, the effects of strain rate can be predicted from the EYSM by

$$\Delta T_r = T_{rd} - T_{rs}, \text{ where } \sigma_y(\dot{\varepsilon}_s, T_{rs}) = \sigma_y(\dot{\varepsilon}_d, T_{rd}) \qquad (4)$$

and the "d" and "s" subscripts refer to dynamic and static conditions, respectively. In all cases the agreement between predicted and measured values is quite good, supporting both the assumptions and the physics underlying the EYSM.

SUMMARY AND CONCLUSIONS

In summary, the data and analysis presented here demonstrate that the program heat of V-4Cr-4Ti undergoes a "normal" stress-controlled ductile-to-cleavage transition, typical of bcc alloys. The temperature delineating this transition is shifted by irradiation hardening by an amount that is predictable by an equivalent yield stress model. This demonstrates the primary role of irradiation hardening in embrittlement of these alloys, and strongly contradicts alternate *ad hoc* explanations (e.g., impurity pickup).

ACKNOWLEDGMENTS

This work was supported in part by the Office of Fusion Energy, DOE, Grant No. DE-FG03-87ER-52143.

REFERENCES

1. Loomis, B.A., Smith, D. L., J. Nucl. Mater., Vols. 179-181, 1991, p 783.
2. Loomis, B.A., Smith, D. L., Garner, F. A., ibid., p 771.
3. Chung, H. and Smith, D. L., J. Nucl. Mater., Vols. 191-194, 1992, p 942.
4. Loomis, B. A., Nowicki, L. J., Gazda, J., Smith, D. L., , DOE/ER-0313/15, March 31, 1993, p 318.
5. Loomis, B. A., Chung, H. M., Nowicki, L. J., Smith, D. L., J. Nucl. Mater., Vols. 212-215, 1994, p 799.
6. Edsinger, K., Odette, G. R., Lucas, G. E., Sheckherd, J. W., J. Nucl. Mater. , Vols. 233-237 (1996) p. 342.
7. Odette, G. R., DOE/ER-0313/20, Department of Energy (1996) 283-298.

8. Chung, H. M., Tsai, H.-C., Smith, D. L., Peterson, R., Curtis, C., Wojcik, R., Kinney, C., DOE/ ER-0313/17, March, 1994.

9. Grossbeck, M. L., Alexander, D. J., Henry, J. J., Eatherly, W. S., Gibson, L. T. DOE/ER-0313/ 18, March 1995.

10. Gubbi, A. N., Rowcliffe, A. F., Eatherly, W. S., ibid.

11. Edsinger, K., PhD Thesis, Department of Chemical Engineering, UCSB, 1996.

12. Edsinger, K., Odette, G. R., Lucas, G. E. Proceedings of the IEA International Symposium on Miniaturized Specimens for Testing Irradiated Materials, KFA Julich, 1995, p 150.

13. Odette, G. R., Donahue, E., Lucas, G. E., Sheckherd, J. W.,DOE/ER-0313/20, Department of Energy (1996) 11-29.

14. Alexander, D. J., Snead, L., Zinkle, S., Gubbi, A., Rowcliffe, A., Bloom, E., ibid. 87.

15. Odette, G. R., J. Nucl. Mater., Vols. 212-215, 1994, p 45.

16. Alexander, D. J., Snead. L., ASTM-STP-1325 (in press).